Adatom-induced spin reorientation transitions and spin canting in Co films on a stepped Cu(001) surface

Takeshi Nakagawa, Hirokazu Watanabe, and Toshihiko Yokoyama*
Department of Molecular Structure, Institute for Molecular Science, and Department of Structural Molecular Science, The Graduate University for Advanced Studies (Sokendai), Myodaiji-cho, Okazaki 444-8585, Japan
(Received 28 June 2006; revised manuscript received 29 August 2006; published 23 October 2006)

We have investigated spin reorientation transitions on ultrathin Co films grown on a stepped Cu(1 1 17) surface upon adsorption of Ag and NO by means of the magneto-optical Kerr effect, the magnetization-induced second harmonic generation, x-ray magnetic circular dichroism, and laser excited photoemission magnetic circular dichroism. Although a spin reorientation transition from the step parallel to perpendicular direction is well known to occur after Ag deposition, the magnetization after the transition is found to be canted from the film plane toward the terrace atomic plane. On the other hand, upon NO adsorption, the Co film is shown to lose its inherent twofold uniaxial magnetic anisotropy without showing canted magnetization.

DOI: 10.1103/PhysRevB.74.134422 PACS number(s): 73.20.At, 68.35.Bs, 71.45.Lr

I. INTRODUCTION

Magnetic anisotropy of thin metal films grown on substrates has been investigated for more than a decade because of both fundamental interest and technological requirements. Lattice mismatch between the magnetic film and the substrate, surface anisotropy, and interface anisotropy settle the direction of the magnetization. The thickness dependency of the anisotropy sometimes results in a spin reorientation transition (SRT). Although a flat magnetic film is likely to show an in-plane magnetic easy axis due to its demagnetization energy, perpendicular magnetization is stabilized due to the complementary terms. Since the balance between the different anisotropies is subtle, the various surface modifications by adatoms drive SRT such as in Ni/Cu(001) (Refs. 1–6) and Co/Pd(111).[7,8]

Step surfaces bring additional magnetic anisotropy within the surface plane since the directions parallel and perpendicular to the step edge are no longer equivalent. It is found that Co on stepped Cu(001) surfaces gives a magnetic easy axis parallel to the step.[9–18] A double hysteresis loop is observed in magnetic films on stepped surfaces, while a normal rectangular shaped hysteresis is detected along the easy axis [see Fig. 2(a)]. The double hysteresis loop is phenomelogically attributed to the magnetic anisotropy from atoms located at step sites.[11] From a microscopic point of view, Dhesi *et al.*[19] have evaluated the spin-orbit coupling by means of the x-ray magnetic linear dichroism measurements. They have shown that the spin-orbit coupling parallel to the step is larger than the one perpendicular to the step and have given a quantitative comparison between the anisotropic spin-orbit coupling and magnetocrystalline anisotropy. Although the magnetic anisotropy due to the step edge seems quite strong and thus hard to be reoriented, Weber *et al.*[17,18] discovered adatom induced SRT on Co/Cu(1 1 41) from the $\parallel$ step to the $\perp$ step direction. Adsorption of Ag, O, and Cu on the step edge sites changes the step magnetic anisotropy, resulting in SRT.

Beside the twofold symmetry in the step surface, the breaking inversion symmetry perpendicular to the step gives canted magnetization toward the surface normal. Mikuszeit *et al.*[16] have found canted magnetization on Co/Cu(1 1 13) by means of MOKE (magneto-optical Kerr effect) measurements. They have evaluated that the canting angle is 6.6° at the thinnest limit, which corresponds to the angle between the film and atom terrace planes of Cu(1 1 13); namely the magnetization is aligned within the atom plane. Although their measurement on canted magnetization is highly reliable, they have performed the experiments basically along the hard axis perpendicular to the step, and the magnetization of 4 ML Co was not able to be saturated because of too strong uniaxial anisotropy. It is thus interesting to investigate possible canted magnetization of Ag-deposited thin Co films that shows a $\perp$ step easy axis.[17,18]

In the present work, we have investigated magnetic properties of Ag- and NO-covered Co films on Cu(1 1 17) by means of MOKE, x-ray magnetic circular dichroism (XMCD), the magnetization-induced second harmonic generation (MSHG), and laser excited photoelectric magnetic circular dichroism (MCD). The main subject is to evaluate canted magnetization on Ag- and NO-covered Co films. For Ag/Co/Cu(1 1 17) canted magnetization is observed with high accuracy using XMCD. The variation of the orbital magnetic moments before and after Ag deposition is also estimated in order to discuss the role of the orbital magnetic moments in the SRT.[19–22] Moreover, magnetization curves taken with the MSHG method are shown to discuss the technical magnetization process. On the other hand, NO adsorption induces a loss of inherent twofold uniaxial anisotropy, resulting in a fourfold symmetric film, and no canted magnetization is found.

II. EXPERIMENTS

The experiments were performed in an ultrahigh vacuum (UHV) chamber and its base pressure was 2×10^{-10} Torr. The chamber was equipped with low energy electron diffraction (LEED) and an electromagnet. The LEED equipment was also used for Auger electron spectroscopy (AES). A Cu(1 1 17) surface was cleaned by repeated cycles of Ar^+ sputtering at 1 keV and subsequent annealing at 875 K for

10 min. The cleanliness and order were verified by LEED, AES, and x-ray absorption spectroscopic (XAS) measurements. Co and Ag were deposited from commercial evaporators, and the pressure was maintained below 5×10^{-10} and 2×10^{-9} Torr during Co and Ag deposition, respectively. The sample temperature was kept at 300 K for Co and Ag depositions, while NO is adsorbed at 90 K to avoid dissociation of molecules. All measurements for Co films after Ag deposition and NO adsorption were done at 300 K and 90 K, respectively. The Co coverage was calibrated by AES and XAS. Scanning tunneling microscopy (STM) from Unisoku with electrochemically etched W tips was used for the study of the film morphology. In the STM measurements, we employed a Cu(1 1 41) crystal instead of Cu(1 1 17), which shows essentially the same magnetic properties including Ag- and NO-covered Co films.

Magnetization curves were taken with MOKE and MSHG. The longitudinal MOKE experiment was performed using a diode laser (635 nm, CW, 5 mW).[4] The light incidence and reflection angles were set at 45°. The MSHG measurements were conducted using a similar system in the literature.[23] A Ti:sapphire laser was used as an excitation source (800 nm, 80 MHz, 100 fs, Spectra Physics).

The Co *L*-edge XMCD measurements were carried out at Beamline 4B of UVSOR-II in Institute for Molecular Science.[4,24] The energy resolution was $E/\Delta E\sim1000$. During the XMCD measurements, a magnetic field of ±2500 Oe was applied, which was large enough to saturate the magnetization along the in-plane easy and hard axes, but was not sufficient for the hardest axis along the surface normal. The spectra were recorded by measuring the sample drain current (total electron yield) and by flipping the magnetic field or the x-ray helicity. In order to extract the XMCD spectra, the subtracted spectra were divided by the correction factor of $P_c \sin\theta_i$ (θ_i is the x-ray incidence angle with respect to surface normal), and moreover, a so-called self-absorption effect[25] was taken into account with the assumption of the electron escape depth of 25 Å and the unform film thickness. The absorption coefficients were taken from the literature table.[26]

In order to determine the magnetic easy axis including the perpendicular component precisely, incident angle dependence of MCD was investigated in remanent magnetization. In case of Ag deposition, we employed XMCD. The XMCD signal becomes zero when the magnetization **M** is perpendicular to the light helicity. By varying the polar angle of the sample crystal, the XMCD signals at the L_{III} peak top were recorded. The accuracy of the incident angle was verified by the laser reflection and was estimated as less than 0.5° at most. In case of NO/Co/Cu(1 1 17), due to unfortunate lack of the beam time at Beamline 4B, we employed a laser-excited photoelectric MCD method[27,28] instead. We employed the same laser diode as for the MOKE measurements. In order to overcome the work function, Cs was deposited on the surface. We will assume here that Cs does not meaningfully affect the magnetic properties of NO/Co/Cu(1 1 17) since no significant changes were observed in the longitudinal MOKE measurements before and after Cs deposition.

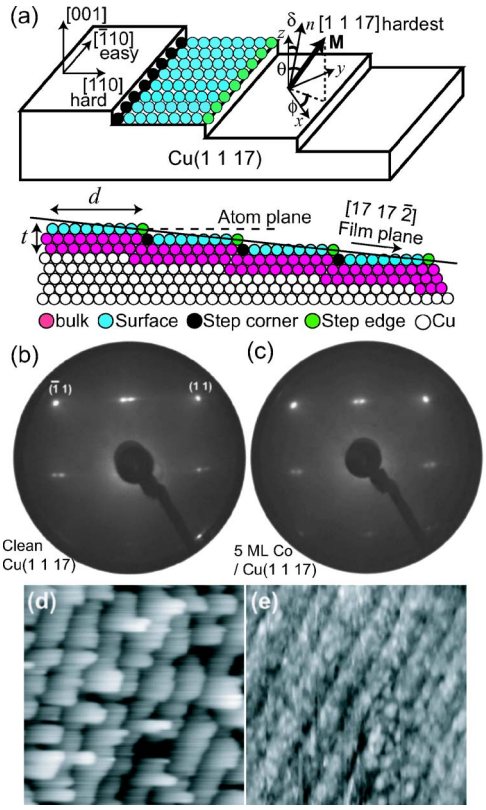

FIG. 1. (Color online) (a) Model surface structure of a Co film on Cu(1 1 17); (b), (c) the LEED patterns with the primary electron energy of 127 eV before (b) and after (c) 5 ML Co deposition. The STM images (40×40 nm^2) of (d) clean 3 ML/Cu(1 1 41) and (e) NO-adsorbed 3 ML Co/Cu(1 1 41). V_s=0.3 V; I_t=0.15 nA.

III. RESULTS AND DISCUSSION

A. Clean Co films

We will first show the experimental results on clean Co films on Cu(1 1 17). Figure 1(a) shows a model surface structure. The terrace is 8.5 atom wide, and is separated by a monoatomic step. The Co atoms are classified into four kinds: bulk, surface, step corner, and step edge atoms.[11] For the Co/Cu(1 1 17) film, the ∥ step direction is known as a magnetic easy axis, the ⊥ step direction is a hard axis, and the direction perpendicular to the surface is the hardest axis. Figures 1(b) and 1(c) show the experimentally observed LEED patterns before and after Co deposition, respectively. The fundamental spots clearly split into two after Co deposition as well, confirming that the Co film grows in a layer-by-layer fashion and the step edge is maintained on the Co film surface. The STM image of Co(3 ML)/Cu(1 1 41) in Fig. 1(d) also shows the maintenance of the step array after deposition.

Figure 2 shows the results of MOKE, MSHG, and XMCD on clean Co on Cu(1 1 17). In the longitudinal MOKE of Fig. 2(a), the magnetization hysteresis curve along the ∥ step direction is a simple rectangular shape, while the ⊥ one shows zero remanence and a double hysteresis loop with the shift field of ~220 Oe. Figure 2(b) shows the Co *L*-edge XMCD spectra of 3 ML Co on Cu(1 1 17) with **M**∥step and

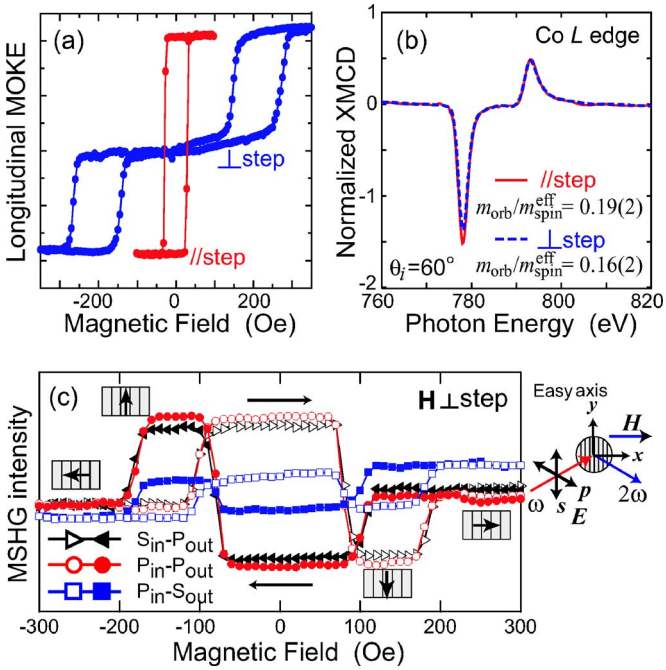

FIG. 2. (Color online) (a) Longitudinal MOKE magnetization hysteresis curves of 5 ML Co on Cu(1 1 17) with **H**∥step and **H**⊥step. (b) Grazing incidence Co *L*-edge XMCD spectra of 3 ML Co on Cu(1 1 17) with **M**∥step and **M**⊥step. (c) MSHG magnetization hysteresis curves of Co(5 ML)/Cu(1 1 17) with **H**⊥step. Polarization dependence is also given; for instance S_{in}-P_{out} denotes the *s*-polarized incident fundamental light and the *p*-polarized generated second harmonics. Also shown are the scan directions of the magnetic field, and the schematic magnetization direction during the technical magnetization.

M⊥step. As seen in the L_{III} edge around 779 eV in Fig. 2(b), the ∥ step intensity is larger than the ⊥ step one, while the L_{II}-edge XMCD intensities are nearly the same. From the sum rule,[31] the larger L_{III} XMCD is ascribed to a larger orbital magnetic moment in the ∥ step direction than that in the ⊥ step direction. A quantitative sum-rule analysis[31,32] yields the orbital and effective spin magnetic moments, m_{orb} and m_{spin}^{eff}. The effective spin magnetic moment m_{spin}^{eff} is given as $m_{spin}^{eff}=m_{spin}+7m_T$, where m_{spin} is the real spin magnetic moment and m_T the magnetic dipole term.[32] The numerical results of the ratio, m_{orb}/m_{spin}^{eff} are indicated in Fig. 2(b) since the m_{spin}^{eff} values show no difference between the ∥ step and the ⊥ step. Although the difference of the ratio between the ∥ step and ⊥ step directions are also not so significant, the ∥ step direction shows larger orbital magnetic moments, as can be expected from the spectra. According to the well known concept given by Bruno,[33] the present finding is consistent with the fact that the magnetic easy axis isparallel to the step edge.

In Fig. 2(c), we show the MSHG results that were recorded with **H**⊥step. Three polarization dependences of S_{in}-P_{out}, P_{in}-P_{out}, and P_{in}-S_{out} are given. We examined the S_{in}-S_{out} polarization as well, but omit it in Fig. 2(c) since no meaningful hysteresis was obtained (only a straight background). The features of the polarization dependent magnetization curves are considerably different from those of MOKE and it is worth discussing what we observe. Here, we can recall the selection rule in MSHG.[29] When the Cartesian coordinate is defined as in Fig. 2(c) (note that the definition is different from that of Fig. 1), nonzero elements of a rank-3 tensor that are responsible for the second harmonic generation from the fcc(001) surface are tabulated in the literature.[29] Although the present system is slightly inclined from the ideal (001) surface and more nonzero elements appear, simple description of the (001) surface is sufficient for the following qualitative discussion on the features of the magnetization curves.

In the P_{in}-S_{out} configuration, when **M**∥*x* (longitudinal), there exist nonzero *yxx* and *yzz* terms, which are odd functions with respect to **M**. On the contrary, all the even and odd terms vanish when **M**∥*y* (transverse), which implies that the P_{in}-S_{out} MSHG shows a similar magnetization curve to that of longitudinal MOKE. Actually in Fig. 2(c), a double hysteresis loop emerges. The different shift field in MSHG from the MOKE result in Fig. 2(a) is caused by slight differences in the sample qualities such as the differences of the long-range order of the crystal and/or the contamination on the film surface. On the other hand, in the S_{in}-P_{out} configurations, when **M**∥*x*, the even *zyy* term is nonzero but there remains no odd term, while the odd *xyy* and the even *zyy* terms are nonzero when **M**∥*y*. The P_{in}-P_{out} configuration is similar to the S_{in}-P_{out} one. Only the even *xzx*, *zxx*, and *zzz* terms are nonzero when **M**∥*x*, while the odd *zzx*, *xxx*, *xzz* and the even *xzx*, *zxx*, and *zzz* terms are nonzero when **M**∥*y*. Since only the transverse contribution contains odd terms in the S_{in}-P_{out} and P_{in}-P_{out} configurations, MSHG gives a magnetization hysteresis curve perpendicular to **H** (*y* axis). Actually, the signal intensities at ±300 Oe are almost equivalent to each other and the longitudinal contribution is thus quite small. The observed features from −200 to +200 Oe are thus ascribed to the transverse magnetization.

We can consequently get information on the magnetization reversal process including the transverse direction. When we start from $H=+300$ Oe, the magnetization **M** is completely aligned to **H** (+*x*, hard axis). With decreasing *H*, **M** turns downwards (−*y*, easy axis) at $H=+100$ Oe. At $H=-100$ Oe, **M** is once reversed to the upward direction (+*y*, easy axis), and at $H=-200$ Oe **M** is resultantly aligned to the left (−*x*, hard axis). Although the MSHG technique is usually emphasized to be surface sensitive,[30] it also allows us to extract the transverse Kerr-like effect without changing the experimental configuration, which is useful in investigating technical magnetization processes of ultrathin films.

B. Ag-deposited Co films

Figures 3(a) and 3(c) show the magnetization curves recorded by the longitudinal MOKE and the polarization dependent MSHG of Ag(1 ML)-deposited 5 ML Co on Cu(1 1 17). In contrast to the results of the clean Co films, the ⊥ step magnetization curve shows a simple rectangular shape, while the ∥ step gives a double hysteresis loop with the shift field of ~200 Oe. This observation implies that the magnetic easy axis is perpendicular to the step within the film plane and that SRT actually occurs upon Ag deposition.

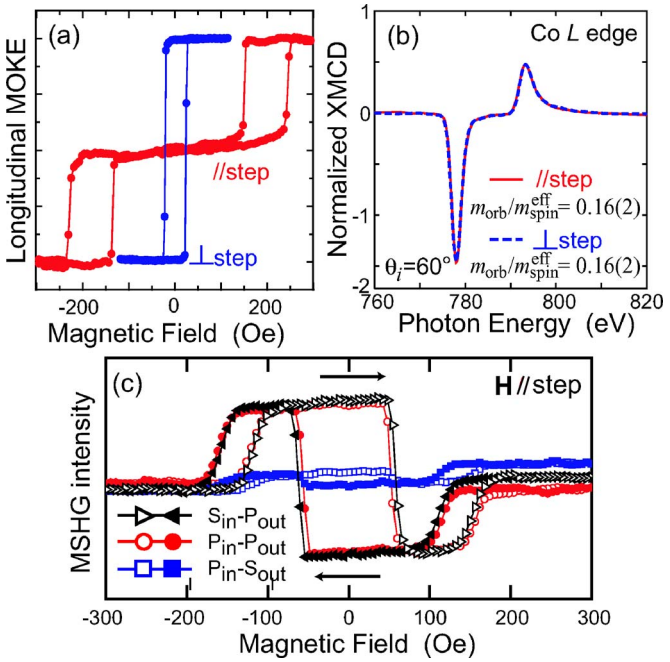

FIG. 3. (Color online) (a) Longitudinal MOKE magnetization hysteresis curves of 1 ML Ag-deposited 5 ML Co on Cu(1 1 17) with $\mathbf{H}\|$step and $\mathbf{H}\perp$step. (b) Grazing incidence Co L-edge XMCD spectra of Ag-deposited 3 ML Co on Cu(1 1 17) with $\mathbf{M}\|$step and $\mathbf{M}\perp$step. (c) MSHG magnetization curves of Ag(1 ML)/Co(5 ML)/Cu(1 1 17) with $\mathbf{H}\|$step. Polarization dependence is also given.

Our result confirms the previous SRT in Co/Cu(1 1 41) by Weber *et al.*[17,18] although the magnetic anisotropy is larger in Co/Cu(1 1 17). The MSHG magnetization curves exhibit similar features to those of the clean Co films in Fig. 2(c). The magnetization reversal process should be essentially the same as the above case, although the easy axis is rotated from the ∥ step to ⊥ step direction by 90°. Figure 3(b) shows the Co L-edge XMCD spectra of Ag(1 ML)/Co(3 ML)/Cu(1 1 17). There can be seen almost no difference between the ∥ step and ⊥ step spectra. From the sum rule analysis given in the figure, the ratio of m_{orb}/m_{spin}^{eff} is actually equivalent. When one compares the results with those of the clean ones, one can find that the ∥ step orbital magnetic moment is suppressed, while the ⊥ step one is unchanged. Although these results cannot conclude the magnetic easy axis, it is not contradictory to the occurrence of the SRT possibly because the difference is too small to detect by XMCD.

Next we will discuss the possibility of canted magnetization. We have measured the canting angle of the Ag/Co/Cu(1 1 17) using the XMCD technique. Figure 4 shows the incident angle dependence of the Co L_{III}-edge XMCD intensity at the peak top energy. In the case of clean Co, where the magnetic easy axis is along the step edge, the intercept is found at θ_i=0°, in agreement with the fact that the easy axis lies on the film plane with no canting. On depositing Ag, the easy axis turns to the ⊥ step direction even at 0.2 ML Ag, which is approximately equal to the density of the steps. According to the previous work,[18] the Ag atoms adsorb at the step edges, which modifies the magnetic anisotropy at Co atoms at the step, resulting in the SRT.

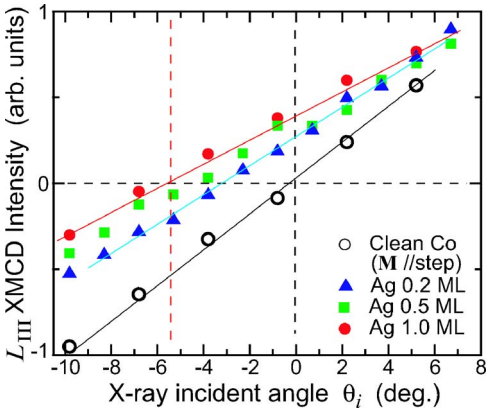

FIG. 4. (Color online) Incident angle dependence of Co L_{III}-edge XMCD at the peak top energy for clean 5 ML Co and Ag(0.2, 0.5, and 1.0 ML)-deposited 5 ML Co on Cu(1 1 17). The zero (−4.8) degree corresponds to the angle perpendicular to the film (atom) plane. In the case of the clean Co film, the magnetization is parallel to the step edge, while all the Ag-deposited Co give magnetic easy axes perpendicular to the step.

As the coverage of Ag increases, the intercept is shifted to the negative side that corresponds to the magnetization canting from the film plane to the atom plane (see Fig. 1). The canting angle at 1 ML Ag is estimated as ~5.5±0.5°, which is approximately equivalent to the angle between the film and atom planes of 4.76° of Cu(1 1 17). The magnetization thereby is close to the atom plane, and lifted up toward the surface normal direction. In the previous work by Mikuszeit *et al.*,[16] it was concluded that the direction of canted magnetization approaches the atomic plane at the thinnest limit, which seems in accordance with the present work. It should be noted that Mikuszeit *et al.*[16] have measured the spin canting on Co/Cu(1 1 13) along the hard axis with the magnetic field applied to saturate the magnetization.

C. NO-adsorbed Co films

Figure 5(a) shows the magnetic hysteresis curves of the 6 ML Co film after the dosage of a saturated amount of NO [$3L(L=10^{-6}$ Torr s)] at 90 K, recorded with the longitudinal MOKE method. The hysteresis loops are completely identical between the ∥ step and ⊥ step directions. The step induced anisotropy vanishes and the film behaves as if the film symmetry is fourfold. Figure 5(b) gives the variation of the shift field as a function of NO exposure. There can be found no abrupt decrease in the shift field, which is gradually suppressed with increasing the NO coverage. The gradual decrease of the shift field indicates that the NO adsorbs uniformly on the surface, not restricted to the step edge, which is supported by the STM observation in Fig. 2(b), showing uniformly adsorbed NO. The different adsorption behavior between Ag and NO may result in the difference in the SRT and the canting angle. Figure 5(c) shows the grazing incidence Co L-edge XMCD spectra of NO-adsorbed 6 ML Co on Cu(1 1 17) with $\mathbf{M}\|$step and $\mathbf{M}\perp$step. One can find almost identical XMCD spectra between the two directions. This indicates that the two axis is equivalent, in agreement

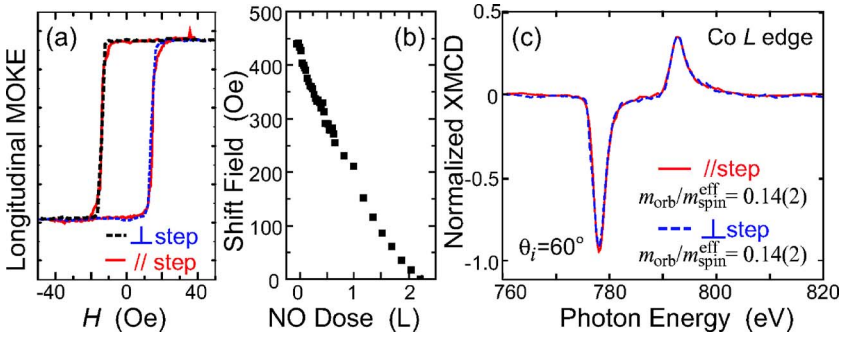

FIG. 5. (Color online) (a) Longitudinal MOKE magnetization hysteresis curves of 3 L NO adsorbed 6 ML Co on Cu(1 1 17) with **H**∥step and **H**⊥step. (b) Variation of the shift field as a function of NO exposure. (c) Grazing incidence Co *L*-edge XMCD spectra of NO-adsorbed 6 ML Co on Cu(1 1 17) with **M**⊥step and **M**∥step.

with the longitudinal MOKE results. Note also that the XMCD intensity is noticeably suppressed compared to those of clean and Ag-deposited films (see Figs. 2 and 3).

We have similarly examined canted magnetization in the NO-adsorbed 5 ML Co film. The measurement method is different from the one in the Ag-deposited film, and the laser excited photoelectric MCD was recorded as a function of the incident polar angle θ_i. Figure 6(a) shows the magnetization hysteresis curve. Although in the present sample there remains still some shift field and the transition is not completed, it may be less important to measure the canting angle in the surface normal direction. To ensure that the magnetization is in the single domain, we measured the canting angle under 300 Oe. Figure 6(b) gives the incident angle dependence. It is clearly found that the MCD asymmetry vanishes exactly at the normal incidence and that the magnetization is lying on the film plane. The result of the NO adsorbed film is in good contrast to that of the Ag-deposited one.

D. Magnetic anisotropy

We will finally discuss the magnetic anisotropy observed in the present systems of Ag- and NO-covered Co films on Cu(1 1 17). According to the Néel model,[11,34,35] the difference of the magnetic anisotropic energies ΔE_a between M∥step and M⊥step (within the film plane) is expressed within the fourth order as

$$\Delta E_a = -\left(K_{2v} + \frac{K_{2s}}{t} + \frac{K_{2se}}{tw} + \frac{K_{2sc}}{tw}\right)\sin^2\delta + K_{4v}\sin^4\delta - \frac{K_{4se}}{tw}(1+\cos^2\delta) + \frac{K_{4sc}}{tw}\sin 2\delta,$$

where t is the thickness of the film, w is the width of the terrace, and δ is the angle between the film and atom planes. In the anisotropic constants K, subscripts 2 and 4 denote the second and fourth orders, while subscripts s, v, se, and sc correspond to the surface, volume, step-edge, and step-corner atoms, respectively. In this equation, since the third term that originates from $K_{4se}(>0)$ is apparently dominant, the ∥ step direction is consequently a magnetic easy axis in clean Co films.

Upon adsorption of NO, the Co film seems to lose twofold step-induced magnetic anisotropy and the magnetic easy axis lies on the film plane as in the clean film. This means that the above ΔE_a is essentially zero. Although the adsorption geometry of NO on stepped Co surfaces is not known, the present STM image indicates uniform adsorption of NO; NO adsorbs on both the step edge and terrace atoms. Since NO adsorption quenches the orbital magnetic moments of the adsorbed Co atoms, the surface and step edge anisotropies should be suppressed. The present observation of the loss of the step induced anisotropy is thus quite reasonable.

On the other hand, Ag deposition induces the transition of the magnetic easy axis from the ∥ step to the ⊥ step direction. Since Ag atoms interact predominantly with the step edge Co atoms, the step edge anisotropy is suppressed, while the step corner anisotropy may be less influenced due to weaker interaction with Ag. This argument can partly explain the SRT. The magnetization is however found to lie closely on the atom plane in Ag/Co/Cu(1 1 17). The energy difference between the **M**∥step and **M**⊥step (within the atom plane) is given as

$$\Delta E_a = -2\pi \mathbf{M}_s^2 \sin^2\delta - \frac{2K_{4se}}{tw}.$$

The energy difference is always negative as long as K_{4se} is positive. Skomski *et al.*[13] discussed unidirectional anisotropy on Co/Cu(1 1 17) based on the experimental observations of the unambiguous unidirectional shift.[14,15] This is not predicted by the Néel model, because the contribution from the step corner atoms is canceled on the atom plane. The situation of the present observation is quite similar to the previous

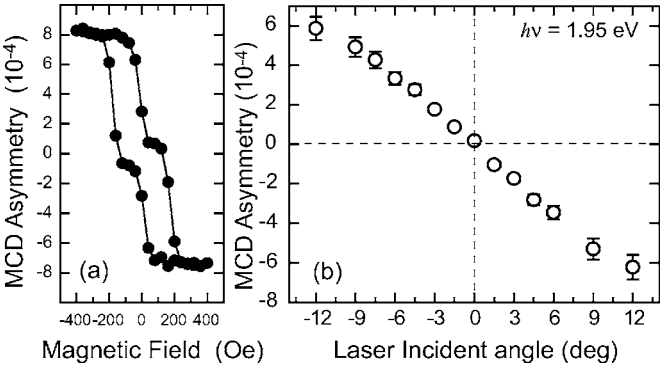

FIG. 6. (a) Magnetization hysteresis curve of NO-adsorbed 5 ML Co on Cu(1 1 17) at 90 K recorded with the laser-induced photoelectric MCD method. (b) Incident angle dependence of the nearly normal incidence laser photoelectric MCD for NO-adsorbed 5 ML Coon Cu(1 1 17) at 90 K. The remanent magnetization was nearly aligned to the ⊥ step direction. The zero (−4.8) degree corresponds to the angle perpendicular to the film (atom) plane.

case and the physical origin of the canted magnetization cannot be explained by the Néel model. In isolated nanowire systems on substrates as well, similar magnetic anisotropy was reported[36,37] and was partly understood theoretically.[38] The one-dimensional Co atomic wires on Pt(997) show an inclined magnetic easy axis. The understanding of the magnetic easy axis of Ag/Co/Cu(1 1 17) needs further quantum-mechanical works.

IV. CONCLUSIONS

We have investigated SRT on Co films on vicinal Cu(1 1 17) upon Ag deposition and NO adsorption. On clean Co films, which show the ∥ step magnetic easy axis, interesting information on the technical magnetization process is obtained from the MSHG measurements. XMCD confirms that the orbital magnetic moment is slightly larger along the ∥ step direction than the ⊥ step one. After depositing of Ag on the Co films, where Ag adsorbs predominantly at the step edge and the SRT from the ∥ step to the ⊥ step direction takes place, the canted magnetization is observed with respect to the films plane; the obtained canting angle indicates that the magnetization lies on the atom plane instead of the inherent film plane. The magnetic anisotropy model by Néel fails in explaining the observation of the canted magnetization, and the physical mechanism requires future theoretical works. On NO adsorption, it is found that NO molecules locate on both the step edge and terrace atoms and the Co film loses the twofold uniaxial magnetic anisotropy. No canting angle is observed for NO adsorption, leaving the magnetization on the film plane. The confinement of the magnetization in the film plane can be explained within the Néel anisotropy model.

*Electronic address: yokoyama@ims.ac.jp

[1] R. Vollmer, Th. Gutjahr-Löser, J. Kirschner, S. van Dijken, and B. Poelsema, Phys. Rev. B **60**, 6277 (1999).
[2] S. van Dijken, R. Vollmer, B. Poelsema, and J. Kirshner, J. Magn. Magn. Mater. **210**, 316 (2000).
[3] J. Hong, R. Q. Wu, J. Lindner, E. Kosubek, and K. Baberschke, Phys. Rev. Lett. **92**, 147202 (2004).
[4] T. Nakagawa, H. Watanabe, and T. Yokoyama, Phys. Rev. B **71**, 235403 (2005).
[5] W. L. O'Brien and B. P. Tonner, Phys. Rev. B **49**, 15370 (1994).
[6] Nakagawa, H. Watanabe, and T. Yokoyama, Surf. Sci. **599**, 262 (2005).
[7] D. Matsumura, T. Yokoyama, K. Amemiya, S. Kitagawa, and T. Ohta, Phys. Rev. B **66**, 024402 (2002).
[8] T. Yokoyama, D. Matsumura, K. Amemiya, S. Kitagawa, N. Suzuki, and T. Ohta, J. Phys.: Condens. Matter **15**, S537 (2003).
[9] A. Berger, U. Linke, and H. P. Oepen, Phys. Rev. Lett. **68**, 839 (1992).
[10] H. P. Oepen, C. M. Schneider, D. S. Chuang, C. A. Ballentine, and R. C. OHandley, J. Appl. Phys. **73**, 6186 (1993).
[11] D. S. Chuang, C. A. Ballentine, and R. C. O'Handley, Phys. Rev. B **49**, 15084 (1994).
[12] R. K. Kawakami, M. O. Bowen, H. J. Choi, E. J. Escorcia-Aparicio, and Z. Q. Qiu, Phys. Rev. B **58**, R5924 (1998).
[13] R. Skomski, H. P. Oepen, and J. Kirschner, Phys. Rev. B **58**, 11138 (1998).
[14] W. Wulfhekel, S. Knappmann, B. Gehring, and H. P. Oepen, Phys. Rev. B **50**, 16074 (1994).
[15] W. Wulfhekel, S. Knappmann, and H. P. Oepen, J. Appl. Phys. **79**, 988 (1996).
[16] N. Mikuszeit, S. Pütter, and H. P. Oepen, J. Magn. Magn. Mater. **268**, 340 (2004).
[17] W. Weber, C. H. Back, A. Bischof, D. Pescia, and R. Allenspach, Nature (London) **374**, 788 (1995).
[18] W. Weber, C. H. Back, U. Ramsperger, A. Vaterlaus, and R. Allenspach, Phys. Rev. B **52**, R14400 (1995).
[19] S. S. Dhesi, G. van der Laan, E. Dudzik, and A. B. Shick, Phys. Rev. Lett. **87**, 067201 (2001).
[20] H. A. Dürr, G. van der Laan, J. Vogel, G. Panaccione, N. B. Brookes, E. Dudzik, and R. McGrath, Phys. Rev. B **58**, R11853 (1998).
[21] S. S. Dhesi, H. A. Dürr, and G. van der Laan, Phys. Rev. B **59**, 8408 (1999).
[22] C. Boeglin, S. Stanescu, J. P. Deville, P. Ohresser, and N. B. Brookes, Phys. Rev. B **66**, 014439 (2002).
[23] A. Kirilyuk and Th. Rasing, J. Opt. Soc. Am. B **22**, 148 (2005).
[24] T. Gejo, Y. Takata, T. Hatsui, M. Nagasono, H. Oji, N. Kosugi, and E. Shigemasa, Chem. Phys. **289**, 15 (2003).
[25] R. Nakajima, J. Stöhr, and Y. U. Idzerda, Phys. Rev. B **59**, 6421 (1999).
[26] B. L. Henke, E. M. Gullikson, and J. C. Davis, At. Data Nucl. Data Tables **54** 181 (1993).
[27] T. Nakagawa and T. Yokoyama, Phys. Rev. Lett. **96**, 237402 (2006).
[28] T. Nakagawa, T. Yokoyama, M. Hosaka, and M. Katoh (unpublished).
[29] R.-P. Pan, H. D. Wei, and Y. R. Shen, Phys. Rev. B **39**, 1229 (1989).
[30] U. Pustogowa, W. Hübner, and K. H. Bennemann, Phys. Rev. B **49**, 10031 (1994).
[31] B. T. Thole, P. Carra, F. Sette, and G. van der Laan, Phys. Rev. Lett. **68**, 1943 (1992).
[32] P. Carra, B. T. Thole, M. Altarelli, and X. Wang, Phys. Rev. Lett. **70**, 694 (1993).
[33] P. Bruno, Phys. Rev. B **39**, R865 (1989).
[34] L. Néel, J. Phys. Radium **15**, 225 (1954).
[35] S. Chikazumi and C. D. Graham, Jr., *Physics of Ferromagnetism*, 2nd ed. (Oxford University Press, Oxford, 1997).
[36] P. Gambardella, A. Dallmeyer, K. Maiti, M. C. Malagoli, W. Eberhardt, K. Kern, and C. Carbone, Nature (London) **416**, 301 (2002).
[37] P. Gambardella, A. Dallmeyer, K. Maiti, M. C. Malagoli, S. Rusponi, P. Ohresser, W. Eberhardt, C. Carbone, and K. Kern, Phys. Rev. Lett. **93**, 077203 (2004).
[38] J. Dorantes-Dávila and G. M. Pastor, Phys. Rev. Lett. **81**, 208 (1998).